-RESEARCH PAPER-

International Journal of Mining and Geo-Engineering

IJMGE

IJMGE 59-3 (2025) 299-313

DOI: 10.22059/IJMGE.2025.393344.595239

Numerical investigation on the effect of roller screen operating parameters on the mechanical behavior of its rolls in classification of green iron ore pellets through coupled DEM-FEM simulation

Mehrshad Asghari [a], Mohammad Noaparast [a, *] and Mohammad Jahani Chegeni [b]

[a] *School of Mining Engineering, College of Engineering, University of Tehran, Tehran, Iran.*

[b] *Faculty of Mining, Petroleum & Geophysics Engineering, Shahrood University of Technology, Shahrood, Iran.*

Article History:

Received: 12 April 2025.

Revised: 12 May 2025.

Accepted: 17 September 2025.

ABSTRACT

The operational parameters of the roller screen substantially affect the efficiency and mechanical performance of its components, particularly those of the rolls. This study presents, for the first time, extensive coupled simulations employing the discrete element method-finite element method (DEM-FEM) to examine the effects of operating parameters on the mechanical behavior of rolls. This is achieved through the utilization of a realistic geometric model of the green pellets in conjunction with a hysteretic spring elastic-plastic contact model. The investigation revealed that decreasing the undersize gap from 9.75 mm to 9 mm led to increases of 20.27%, 29.71%, and 102.91% in the average force, total deformation, and equivalent stress exerted on the rolls, respectively. Furthermore, coupled DEM-FEM simulation tests of an industrial-scale roller screen were conducted for the first time, and the results obtained were compared with those from laboratory tests. The average force acting on the rolls of the laboratory roller screen was measured at 2.43 N. In contrast, simulations of a full-scale roller screen operating at capacities of 120 t/h and 200 t/h revealed average forces of 34.46 N and 54.06 N, respectively. The average total deformation observed in the rolls of the laboratory roller screen was measured at 4.27E-05 mm. In contrast, under industrial conditions, this deformation increased significantly to 1.89E-02 mm at a processing capacity of 120 t/h, and further escalated to 2.95E-02 mm at a capacity of 200 t/h.

Keywords: *Coupled DEM-FEM simulation, Equivalent stress, Green pellets, Industrial-scale roller screen, Total deformation.*

1. Introduction

In the steelmaking industry, the feed material for pellet furnaces is required to exhibit particular attributes concerning granulation and mechanical properties. These characteristics can be improved through dimensional classification achieved by screening processes. Due to the inherent moisture and adhesive properties of green pellets, coupled with their limited mechanical strength, roller screens present considerable advantages over alternative screening methods, such as vibrating screens, for the classification and screening of these pellets [1–5]. The benefits of this equipment, including its efficiency, substantial capacity for classifying green pellets, low noise output, compact spatial requirements, and ability to transport highly adhesive materials with elevated moisture content while minimizing damage to green pellets, have led to its growing adoption in recent years. This apparatus is especially significant for the preparation of an appropriate feed for induration furnaces within the pelletizing industry. A comprehensive schematic illustrating the operational area of the roller screen is presented in Figure 1 [1–5].

The green pellets generated from the pelletizing disc or drum which vary in size from 6 to 22 mm, are subsequently directed to a roller screen for the purpose of size classification. As depicted in Figure 1, the roller screen comprises multiple rolls of designated diameters, with interstitial gaps engineered to categorize the pellets based on their dimensions. Fine-grained pellets, characterized by a granulation size ranging from 6 to 9.5 mm, are separated from the undersized fraction through a gap of 9.5 mm which accounts for three-quarters of the overall length of the screening apparatus. Pellets classified as product, with granulation sizes ranging from 9.5 to 16 mm, are separated through a 15.5 mm gap located in the final quarter of the screen's length. Additionally, coarse-grained pellets, with sizes from 16 to 22 mm, are also expelled from the terminal section of the screen. Consequently, the classification of green pellets is effectively accomplished by their passage through these designated gaps [5, 6].

1.1. Roll deformation

In the process of classifying green pellets, as depicted in Figure 2, the ongoing collisions of the pellets with the roll surface produce an impact. This results in the pellets applying a sustained force on the surface of the roll. As indicated in Figure 2, F_T denotes the total force exerted. Consequently, the rolls experience continuous loading during the operation of the roller screen.

The application of force F_T to the surface of the roll, as depicted in Figure 3(a), generates a bending stress along the roll's length. This bending stress induces deflection, especially in the central region of the roll. When the stress surpasses the yield strength of the roll material, it results in permanent plastic deformation, leading to a misalignment of the roll's axis during rotation, a condition referred to as run-out [7–10]. This misalignment disrupts the proper alignment of the gap between the rolls, particularly in the undersized section. Such deviation from the initial optimal configuration causes operational disturbances and

* Corresponding author: *Tel. /Fax:* +98 21 88008838, *E-mail address:* noparast@ut.ac.ir (M. Noaparast).

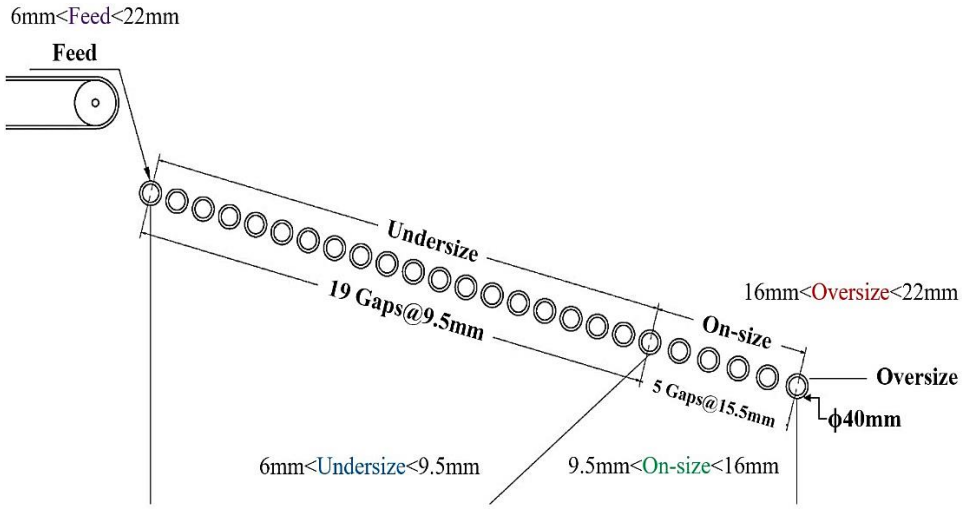

Figure 1. Different operational sections of the laboratory roller screen.

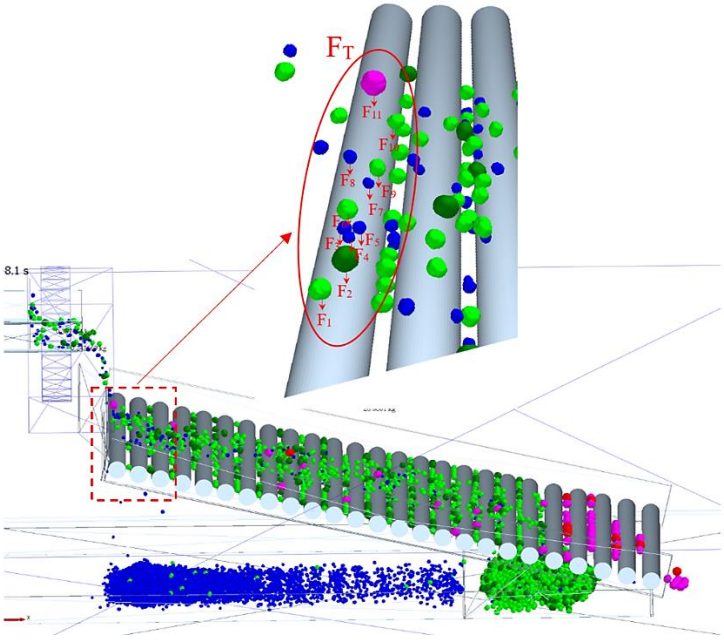

Figure 2. Applied forces due to the impact of pellets on the surface of the roll.

diminishes the efficiency of the screening process [3].

The authors of the current study have conducted investigations and monitoring of an industrial roller screen utilized in a pelletizing plant. The findings regarding the effects of bending on the inter-roll gap are illustrated schematically in Figure 3(b). This illustration demonstrates that the negative impact of bending on roll 4 results in a reduction of the gap on the right side to 9 mm during roll rotation, while the gap on the left side expands to 10 mm. Consequently, the product pellets are directed toward the fine-grain section during the screening process, leading to a quantitative decrease in the roller screen efficiency. Meanwhile, fine-grain pellets are rerouted to the product section. Ultimately, these fine particles are introduced into the induration furnace as feed, resulting in a deterioration of quality. The inclusion of fine particles in the feed material introduced to the furnace adversely affects the permeability of the pelletizing bed, resulting in elevated pressure within the bed. This phenomenon compromises both the quality and mechanical integrity of the fired pellets, contributes to increased dust emissions, escalates fuel consumption within the furnace, and ultimately undermines the operational efficiency of the pelletizing plant [1, 3, 11].

Given the interdependent relationship between the roller screen and both the upstream processes associated with the pelletizing disc (or drum) and the downstream processes linked to the induration furnace, it is essential to prioritize the optimal design, construction, and operational efficiency of the roller screen. This focus is vital for improving the overall productivity of the pelletizing plant [1,4,5,12,13]. The maintenance of a precise gap between the rolls constitutes a critical operational parameter of the roller screen, as it plays a vital role in the separation of fine-grained materials from the final product. This separation process has a substantial impact on both the productivity and performance of the screen, thereby influencing the overall efficiency of the pellet production process.

1.2. DEM simulation

A comprehensive understanding of the roller screening process necessitates investigations at the particle level to examine the interactions between the pellets and the roll surface. Nevertheless,

executing experimental studies on an industrial scale poses considerable difficulties. Furthermore, the implementation of online analyses is frequently deemed unwarranted due to the considerable financial investments required for such systems. While experimental tests yield significant and dependable insights, the intrinsic heterogeneity, discreteness, anisotropy, and complexity of the dynamic behavior of pellets, stemming from interactions among the pellets themselves and between the pellets and rolls, complicate the testing process. Additionally, the intricacies associated with the fabrication of laboratory equipment contribute to the high costs and time demands of these tests. The difficulties associated with executing experimental studies, along with the minimal values of deformation and bending stress, constrain their utility for comprehensive analyses and parametric investigations of roller screening processes [3, 4, 11, 12, 14].

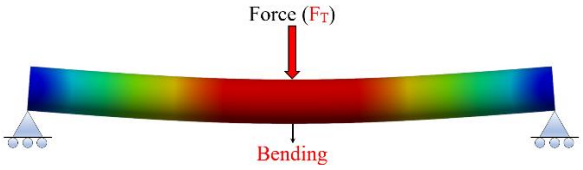

(a) the applied bending stress to the roll along its length.

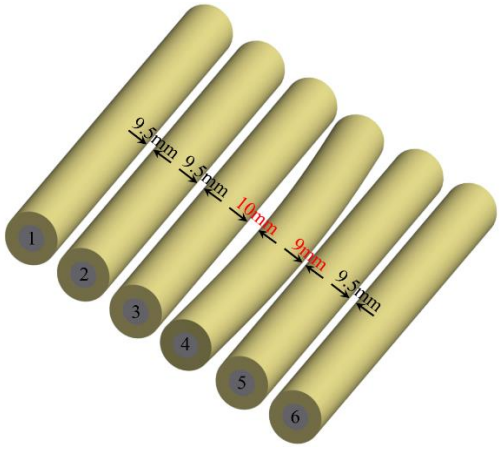

(b) the non-uniformity of gap opening of 9.5 mm between rolls of 3, 4 and 5 in the undersize region because of the roll bending.

Figure 3. The resultant bending stress to the roll while classification of the pellet which causing the gap opening non-uniformity.

The utilization of simulations has emerged as a vital instrument in the design and optimization of industrial processes. Notably, mechanical modeling and numerical simulation, particularly through the discrete element method (DEM), are integral to developmental research [1, 15–19]. In order to investigate the classification behavior of green pellets on a roller screen, it is imperative to accurately calibrate and validate DEM simulations. This methodology allows for the simulation and calculation of the forces exerted by the pellets on the surface of the rolls.

1.3. FEM simulation

In the subsequent phase of the simulation, it is imperative to implement the forces derived from the DEM onto the rolls in order to evaluate their mechanical characteristics which encompass deformation, stress, and bending. Furthermore, it is crucial to analyze the influence of various factors on these parameters. To facilitate this analysis, the Finite Element Method (FEM), a highly regarded and extensively employed numerical program in the field of mechanical engineering, is accordingly utilized. The forces obtained from the DEM are incorporated into the FEM framework to ascertain the mechanical behavior of the rolls [20–25].

1.4. Coupled DEM-FEM simulation

The methodology for transferring communication and data from DEM simulations to FEM simulations is referred to as the DEM-FEM coupling approach. This coupling enables precise simulation of the contact forces produced by the impact of discrete pellets, as well as the subsequent deformation of the roll which is treated as a continuous entity [23, 26–30]. This research utilizes a coupling of DEM and FEM to comprehensively and precisely analyze the mechanical behavior and response of a roller screen roll. The findings are intended to inform decisions that will enhance its structural and functional design. The non-spherical geometry of the pellet, in conjunction with its elastic-plastic characteristics, requires the implementation of a precise model developed through image analysis. This model effectively captures the pellet's morphology and integrates a contact model for the hysteretic spring. The outcomes derived from this model were in alignment with the results from experimental assessments of contact measurements and roller screen tests which facilitated their calibration. A comprehensive overview of previous coupled DEM and FEM simulation studies, encompassing the various types of screens and the parameters investigated is provided in Table 1.

According to Table 1, numerous investigations have been undertaken to explore the influence of operational parameters on the interaction between particles and vibrating screens. These studies have focused on variables such as the impact load exerted by particles on the screen mesh and plate, along with the subsequent distribution of stress and deformation. Nevertheless, to this point, there has been a lack of simulation studies employing FEM and, by extension, coupled DEM-FEM approaches specifically in relation to roller screens, and their functional optimization. Consequently, the current body of simulation research pertaining to roller screens is predominantly confined to the DEM. This research utilizes an innovative methodology that combines DEM with FEM to create a coupled DEM-FEM model for the analysis of the roller screen. After establishing this integration, the study evaluates the deformation and stress experienced by the rolls of the roller screen as a result of the impact load from the pellets during the classification process, while considering variations in the operational parameters of the roller screen. The findings from this analysis will support a parametric study focused on the structural design and optimization of the roller screen.

2. Simulation methods

2.1. Experimental tests of the roller screen

In order to examine the performance of the roller screen in the dimensional separation of green pellets and to evaluate the influence of operational variables on its classification efficacy, a series of extensive experimental tests were performed utilizing the laboratory roller screen depicted in Figure 4, in alignment with the parameters specified in Table 2. Through the execution of these experimental investigations and the establishment of a statistical population pertaining to the dimensional separation of pellets via the roller screen, the resultant data can be employed to assess and refine the results of both the experimental tests and the DEM simulation studies related to the roller screen.

2.2. DEM simulation

2.2.1. Pellet shape modeling

Given the critical influence of the pellet shape on the outcomes of DEM simulations, images of the magnetite pellets utilized in this research which contained 8% moisture and 1% bentonite, were acquired from multiple angles. These images were sourced from experiments aimed at assessing the mechanical properties of the pellets, in addition to experimental roller screen evaluations. The geometric properties of the pellet shape were assessed through the analysis of pellet images utilizing Digimizer software. Following this analysis, the actual shape of the pellet was represented using EDEM software version 2021.2, developed by Edinburgh DEM Solutions [39]. A corresponding pellet

Table 1. Review of performed coupled DEM-FEM simulations of different types of screens with considered parameters.

Type of screen	Investigated parameters	References used	Type of screen	Investigated parameters	References used
Vibrating screen			**Roller screen**		
Flip-Flow	Effect of feed rate on the displacement and stress distribution of screen plate	[31]	No studies have been done in this field.		
Flip-Flow	Effect of excitation angular frequency on the stratification of particles with different size on screen plate	[32]			
Flip-Flow	Effect of relative amplitude, directional amplitude, installation angle and frequency on the particle velocity and applied stress of screen plate	[33]			
Flip-Flow	Effect of material loads on the deformation of screen plate	[23]			
-	– Modeling of interaction between particle-particle and particle-screen – Stress distribution of screen plate	[34]			
-	– Effect of vibration parameters such as amplitude, frequency, vibration direction angle and inclination angle on impact force of particles – Determination of damage, stress and deformation of screen plate	[35]			
-	– Effect of vibration parameters such as amplitude, frequency, vibration direction angle and inclination angle on impact force of particles – Determination of damage, stress and deformation of screen plate	[36]			
linear	– Effect of screening parameters on impact load and sustained stress by particles on screen mesh	[37]			
-	– Effect of impact load by particles on stress and strain of screen structure	[38]			

model was then established to facilitate DEM simulation experiments which encompassed the calibration of contact parameters as well as evaluations of roller screen performance. The findings from these experiments are illustrated in Figures 5 and 6 [40].

Figure 4. The laboratory roller screen for experimental tests of the green pellet classification.

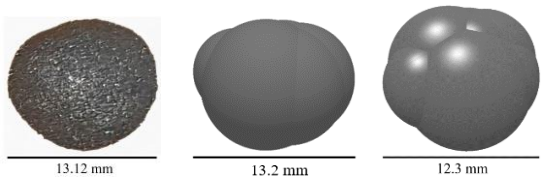

a): real shape of the pellet b): simulated shape of the pellet

Figure 5. Modeling the shape of the magnetite pellet with 8% moisture and 1% bentonite in EDEM [40].

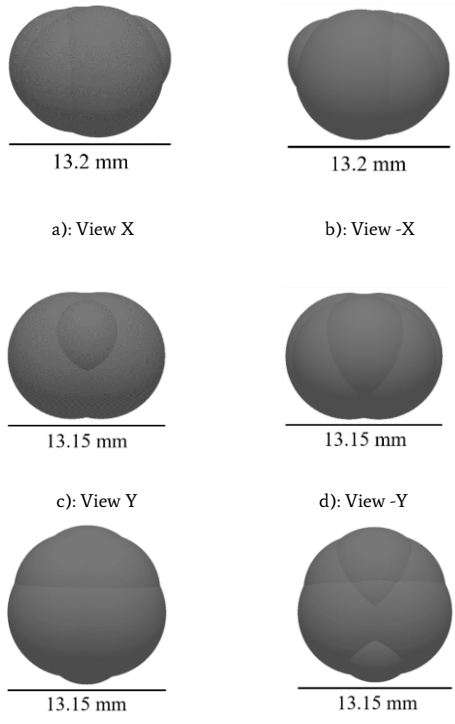

a): View X b): View -X

c): View Y d): View -Y

e): View Z f): View -Z

Figure 6. Modeling the magnetite pellet shape in different views in EDEM under conditions of moisture of 8% and bentonite of 1% [40].

2.2.2. Determination of contact parameters

In order to perform a DEM simulation of the roller screen, the requisite contact parameters were established through empirical methods which involved a series of laboratory experiments. These experiments included drop tests, sliding tests, inclined plane tests, angle of repose tests, and tumbling drum tests. The outcomes of the experimental tests were subsequently compared with the results obtained from DEM simulations in order to assess and calibrate the relevant parameters. The attributes and contact parameters pertaining to pellet-pellet interactions and pellet-geometry (roll) interactions are presented in Table 3. Extensive information regarding the execution of experimental tests and the calibration methodologies employed to ascertain the contact parameters is available in reference [40], scholarly work authored by the researchers involved in this study.

Table 3. Properties and interaction parameters utilized in the EDEM simulation of the roller screen test for magnetite pellets with the actual shape [40].

Parameters		Unit	Values
Pellet properties			
Pellet type		-	Magnetite
Pellet moisture content		%	8
Pellet bentonite dosage		%	1
Pellet density (ρ)		kg/m³	4893
Geometry density (ρ)		kg/m³	1215
Poisson's ratio (ν)-(Pellet; Geometry)		-	0.25; 0.41
Shear modulus (G)-(Pellet; Geometry)		Pa	2.015e+06; 1.02e+08
Pellet yield strength		Pa	0.0554e+06
Pellet shape model		-	Overlapping spheres
Pellet size range		mm	6–22
Test method		-	Bulk pellet
Pellet mass		kg	26, 30, 40, 50 and 70
Feed rate		kg/s	0.417
Time step		s	2.93e-05
Time step		%	20
Simulation time		s	86
Contact parameters			
Physics for interaction	Pellet-pellet	-	Hertz-Mindlin with JKR
	Pellet-geometry	-	Hysteretic spring
Surface energy for the interaction of pellets 6–9.5 mm to pellets 9.5–22 mm		J/m²	1.9
Damping factor		-	-0.0077
Stiffness factor		-	0.125
COR_{P-P}; COR_{P-G}		-	0.104; 0.09
μ_{sP-P}; μ_{sP-G}		-	0.23; 0.6
μ_{rP-P}; μ_{rP-G}		-	0.31; 0.2

[1]COR_{P-P} and COR_{P-G} = coefficient of restitution for pellet-pellet and pellet-roll interactions, respectively.

[2]μ_{sP-P} and μ_{sP-G} = static friction coefficient for pellet-pellet and pellet-roll interactions, respectively.

[3]μ_{rP-P} and μ_{rP-G} = rolling friction coefficient for pellet-pellet and pellet-roll interactions, respectively.

It was determined that green pellets experience elastic-plastic deformation during classification in the roller screening process owing to the forces exerted by the rolls [40]. Consequently, the hysteretic spring contact model, which considers these properties, yields simulation results that are more closely aligned with the outcomes of the experimental tests, thereby demonstrating greater accuracy. Therefore, in this study, coupled DEM-FEM was selected for simulating the pellet-roll interactions, as indicated in Table 3. In contrast, the Hertz-Mindlin model considers only the elastic properties of the pellets, which does not correspond with the experimental test results. The hysteretic spring contact model simulates the mechanical behavior of the green pellet in response to applied forces by incorporating parameters, such as the yield stress and stiffness factor. Consequently, as the magnitude of the forces increased and the resulting stress on the pellet surpassed its yield stress, the pellet experienced a plastic deformation.

2.2.3. DEM simulation of roller screen

The results of the laboratory tests performed on the roller screen indicate the particle size distribution of the input feed utilized in various DEM simulation tests, as illustrated in Figures 7 and 8 [40], which were produced by the authors of this research.

At each time step of the roller screen DEM simulation, as illustrated in Figure 2, multiple pellets collide with each roll. Consequently, the total force exerted on the roll is equal to the sum of the forces exerted by all pellets, as described in Equation (1).

$$F_T = \sum_{i=1}^{n} F_i \quad (1)$$

where:

F_T = the total applied force by collision of pellets to the roll (N)

F_i = the applied force by collision of each pellet to the roll (N)

n = the number of pellets

Extensive laboratory examinations of the roller screen, coupled with the measurement of contact parameters and the execution of corresponding DEM simulation tests, facilitated the evaluation, calibration, and subsequent validation of the results. As a result, the findings from the DEM simulation tests conducted in this research, including force measurements, were assessed and validated in alignment with the study's objectives. Furthermore, these findings were utilized as inputs for FEM analyses.

2.3. Coupled DEM-FEM simulation

Following the execution of DEM simulation tests and the computation of forces exerted on the rolls utilizing EDEM software, it is imperative to incorporate these results as inputs into the FEM simulation framework. This integration serves as the basis for the coupled DEM-FEM simulation approach employed to assess deformation and stress distribution. The algorithm for the coupled DEM-FEM simulation methodology utilized in this research is depicted in Figure 9. For the FEM simulation analyses, ANSYS Workbench software version 2022 R2 was employed.

2.3.1. Modeling roll geometry

The geometric representation of the roller screen, developed utilizing Autodesk Inventor software version 2020, and subsequently imported into ANSYS software, is illustrated in Figure 10. The geometric parameters pertaining to the rolls which are the primary structural elements of the roller screen are comprehensively outlined in Figure 11.

2.3.2. Boundary conditions

A pivotal aspect of coupled DEM and FEM simulations which profoundly influences the outcomes and the validity of the resultant data is the careful consideration of boundary conditions. These conditions govern the application of forces and supports within the simulation framework. Consequently, the identification and specification of these boundary conditions must be executed with meticulous precision and rigor.

- **Remote displacement support**

The parameters for the support employed in the FEM simulation, executed with ANSYS software, were characterized as remote displacement type. A summary of these specifications is presented in Table 4.

- **Applied force methods to the surface of the roll**

The transfer of forces resulting from the impact of the pellet to the surface of the roll was executed through simulations and calculations utilizing EDEM software which were then integrated into ANSYS software using both *.csv format and tabular methods. The details of

these methodologies are presented in Table 5. After conducting DEM simulation tests, in which the force values were calculated at each time step and under various test conditions, the geometry was meshed. Subsequently, a static analysis was performed using ANSYS software, where forces were applied to each roll based on the time steps derived from the DEM tests. The average values of deformation and stress were then reported as the results of each test. Furthermore, the boundary condition encompasses the process of force transfer to the initial roll, referred to as the impact roll where the complete input feed to the screen is initially directed, followed by the subsequent rolls, as depicted in Figures 12(a), (b), and (c).

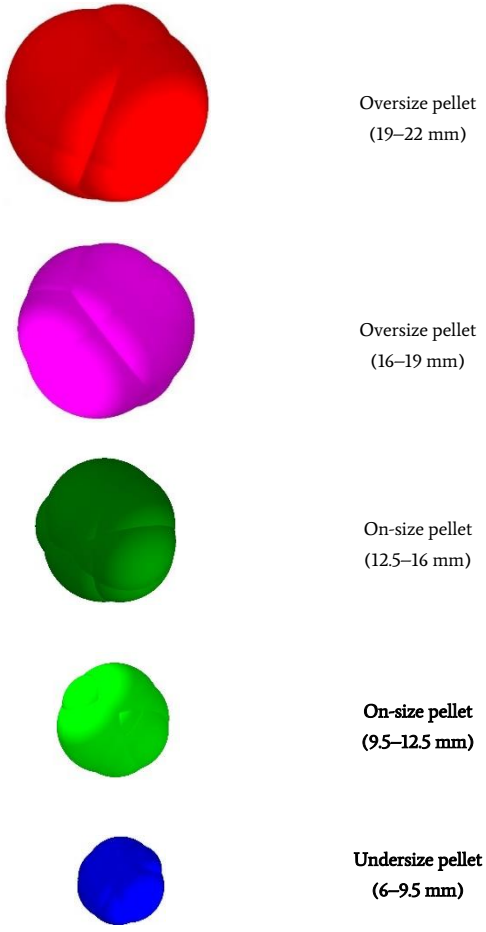

Figure 7. Different particle sizes of the pellet for the DEM simulation of the roller screen [40]

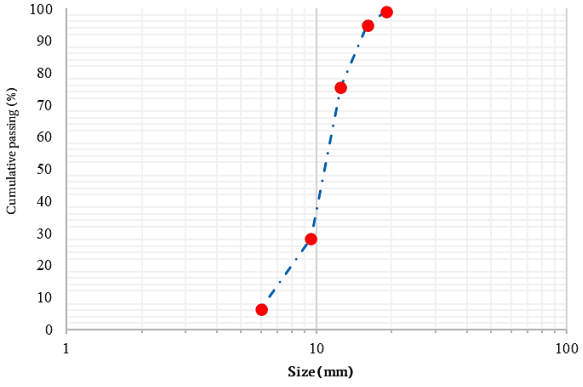

Figure 8. The particle size distribution of the feed for the DEM simulation of the roller screen [40].

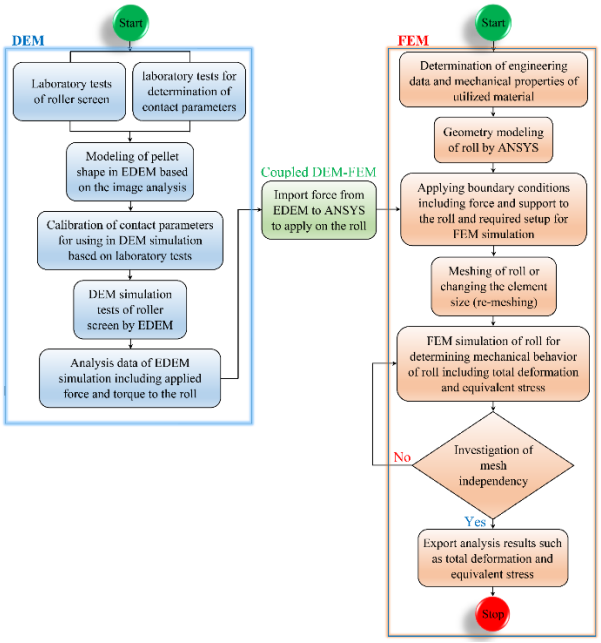

Figure 9. The general algorithm of coupled DEM-FEM principals for the simulation of mechanical properties of the rolls of the roller screen.

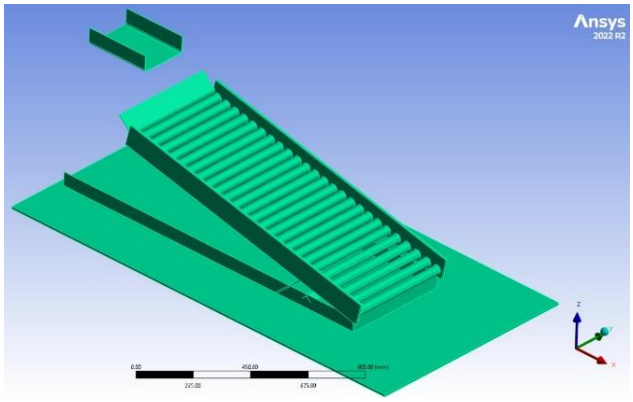

Figure 10. A three-dimensional geometry of the roller screen in the base case prepared by Autodesk Inventor and imported to the ANSYS.

Table 4. Details of the applied remote displacement support.

Parameter	Specification
Scope	
Scoping method	Geometry selection
Geometry	2 Edges
Coordinate system	Global coordinate system
X Coordinate (mm)	-3.7457e-016
Y Coordinate (mm)	240
Z Coordinate (mm)	-4.3194e-016
Definition	
Type	Remote displacement
X Component (mm)	0 (ramped)
Y Component (mm)	0 (ramped)
Z Component (mm)	0 (ramped)
Rotation X (°)	Free
Rotation Y (°)	0 (ramped)
Rotation Z (°)	Free
Suppressed	No
Behavior	Deformable

Table 5. Details of the analysis setting for applying the force by tabular and time step format to the roll surface.

Parameter	Specification
Step controls	
Number of steps	20–85
Auto time stepping	Off
Define by	Time
Time step (S)	1
Solver controls	
Solver type	Program controlled
Weak springs	Off
Solver pivot checking	Off
Large deflection	Off
Inertia relief	Off
Quasi-Static solution	Off

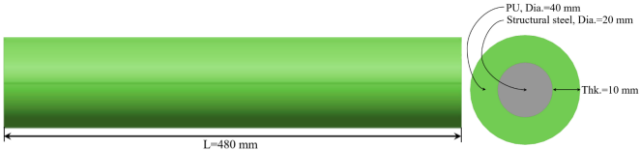

Figure 11. Specification of the roll of the laboratory roller screen.

Based on the experimental and simulation analyses performed on the roller screen (Figure 12(d)), it has been observed that the input load exerted on the surface of the initial roll is distributed in proportion to the width of the chute or conveyor belt that supplies material to the roller screen. As detailed in Table 5, the performance metrics of the roller screen revealed that the number of steps in the FEM simulations varied between 25 and 85. This range reflects the influence of several operational parameters, such as the feeding rate and the results obtained from DEM simulation tests.

2.3.3. Roll meshing

The findings from the research aimed at determining the optimal type of mesh for analyzing the mechanical properties of roller screen rolls are summarized in Tables 6 and 7, which outline the specifications for the different categories of multizone mesh and face mesh.

Table 6. Details of the multizone meshing method for the lateral surface of the roll.

Parameter	Specification
Scope	
Scoping method	Geometry selection
Geometry	2 Bodies
Definition	
Suppressed	No
Method	multizone
Decomposition type	Standard
Mapped mesh type	Hexa
Surface mesh method	Program controlled
Free mesh type	Not allowed
Element order	Use global setting
Source/Target selection	Automatic
Source scoping method	Program controlled
Source	Program controlled
Sweep size behavior	Sweep element size
Sweep element size	Default

2.3.4. Determination of mechanical behaviors of the rolls

As depicted in Figure 9, the coupled DEM-FEM simulation algorithm necessitates the establishment of material engineering specifications, the modeling of the roller screen's roll, the determination of boundary conditions, and the execution of meshing prior to conducting the simulation. This process enables the identification of the required mechanical specifications for the rolls. The principal mechanical properties examined in this study include total deformation and equivalent (von Mises) stress of the roller screen's roll. It is noteworthy that the individual rolls of the roller screen are arranged separately within the overall screen structure. As a result, the coupled DEM-FEM simulation tests were performed independently for each roll. In these simulations, the forces obtained from the DEM analysis were applied to each roll at various time intervals. Consequently, the total deformation and equivalent stress were computed for each time step. The average values of force, total deformation, and equivalent stress, derived from all time steps, represent the simulation outcomes for each roll. By evaluating the mechanical behavior of each roll under varying operational parameters, the average results across all rolls were consolidated to form the final simulation results for the roller screen under the specified operating conditions.

Table 7. Details of the face meshing method for the circular bases of the roll.

Parameter	Specification
Scope	
Scoping method	Geometry selection
Geometry	2 Faces
Definition	
Suppressed	No
Mapped mesh	Yes
Internal number of divisions	Default
Constrain boundary	No

2.4. Investigation of the effect of operational parameters of the roller screen on the applied force and consequently mechanical behaviors of roller screen's rolls

This section provides an in-depth analysis of the influence of different operational parameters of the roller screen, specifically geometric parameters, process parameters, and feed characteristics, on the mechanical behavior of the rolls as observed in the coupled DEM-FEM simulation.

2.4.1. Effect of the undersize gap

Given the substantial importance of the fine-grained area gap as a pivotal factor influencing efficiency and as a fundamental component in the design of the roller screen, this research aims to explore the effects of variations in this parameter on the forces and mechanical properties of the rolls, as detailed in Table 8. The primary goal is to assess how alterations in this parameter impact roll deformation and, subsequently, the run-out phenomenon, with the intention of identifying optimal conditions. To facilitate this analysis, the geometry of the roller screen was modeled using Autodesk Inventor software for a range of undersize gap values, followed by integrated DEM-FEM simulation studies.

2.4.2. Effect of the rotational speed of the rolls

The effects of fluctuations in the rotational speed of the rolls were rigorously investigated utilizing both experimental methodologies and DEM simulations. These studies were carried out at different intervals to evaluate their impact on the efficiency and performance of the roller screen. Consequently, this section provides an analysis of how this parameter influences the deformation and stress experienced by the rolls, as well as the resultant bending phenomenon, in accordance with the conditions specified in Table 9.

Table 8. Study of the undersize gap effect on the coupled DEM-FEM simulation results of roller screen tests.

Feed rate (t/h)	Deck angle (°D)	Roll speed (rpm)	Roll Dia. (mm)	Undersize gap (mm)
3.38	13	225	40	9, 9.25, 9.5 and 9.75

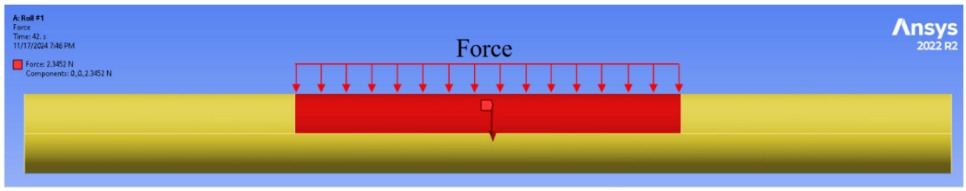

(a)

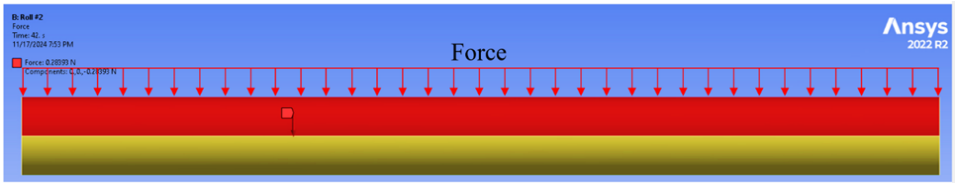

(b)

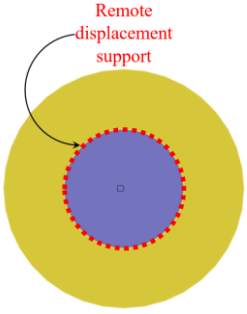

c). the considered remote displacement support.

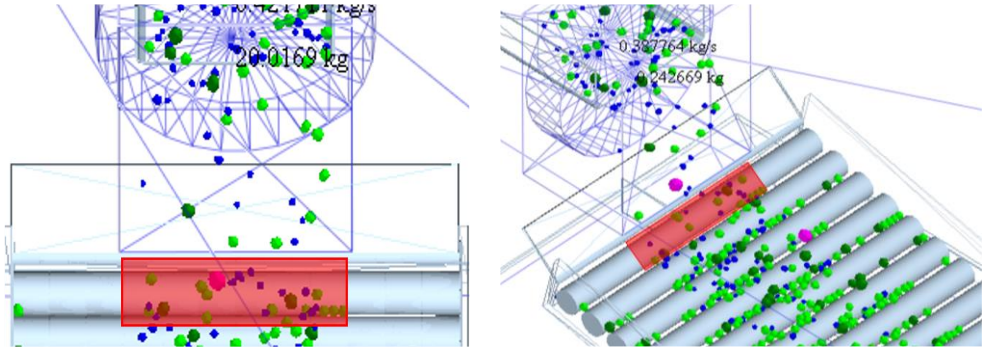

d). applying force to the half surface of the roll 1 equal to the width of the chute or the conveyor belt for transferring the feed to the roller screen according to the practical and DEM simulation tests

Figure 12. Applied boundary conditions for the FEM simulation of the roller screen's roll.

2.4.3. Effect of deck angles

An additional significant factor affecting the forces exerted on the rolls and their deformation during pellet screening tests is the deck angle of the roller screen. Consequently, this section examines the impact of this essential parameter on the mechanical behavior of the rolls and seeks to establish its optimal value. To facilitate this analysis, various roller screen geometries with differing deck angles were developed utilizing Autodesk Inventor and Design Modeler within the ANSYS software version 2022 R2, as depicted in Figure 13. Following this, coupled DEM-FEM simulation tests were performed, as outlined in Table 10.

2.5. Industrial roller screening tests

Following the execution of coupled DEM-FEM simulation tests at a laboratory scale which took into account the structural characteristics of the roller screen under examination as well as process parameters such as the tonnage of the input feed, the subsequent phase involved the modeling of the geometry of the industrial roller screen employed in the pelletizing industry, as demonstrated in Figure 14(a). The geometric model was then simplified, as shown in Figure 14(b). In accordance with the specifications detailed in Figure 14(c) and the experimental conditions specified in Table 11, DEM simulation studies were performed, followed by FEM simulation tests conducted for the first time on an industrial scale for the roller screen, as illustrated in Figure 15. To compare the effects of geometry and, consequently, the capacity of the laboratory and industrial roller screens on the resulting force values and subsequent deformation, all boundary conditions and the method of force application were aligned with those of the laboratory roller screen.

Table 9. Investigation on the impact of the roll speed on the coupled DEM-FEM simulation results of roller screen tests.

Feed rate (t/h)	Deck angle (°D)	Roll Dia. (mm)	Undersize gap (mm)	Roll speed (rpm)
3.38	13	40	9.5	150, 225 and 300

Table 10. Investigation on the impact of deck angles on the coupled DEM-FEM simulation results of roller screen tests.

Feed rate (t/h)	Roll speed (rpm)	Roll Dia. (mm)	Undersize gap (mm)	Deck angle (°D)
3.38	225	40	9.5	10, 13 and 19

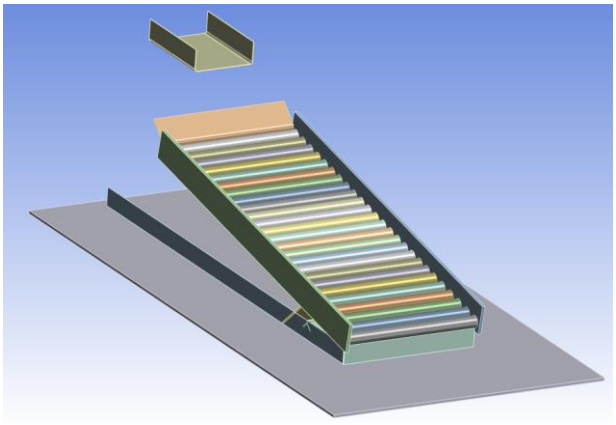

a). the roller screen with the deck angle of 10°.

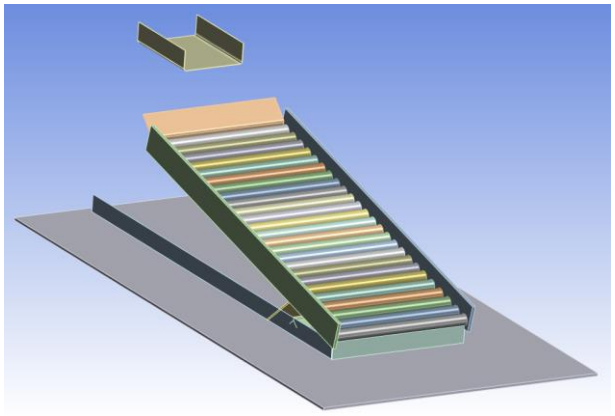

b). the roller screen with the deck angle of 13°.

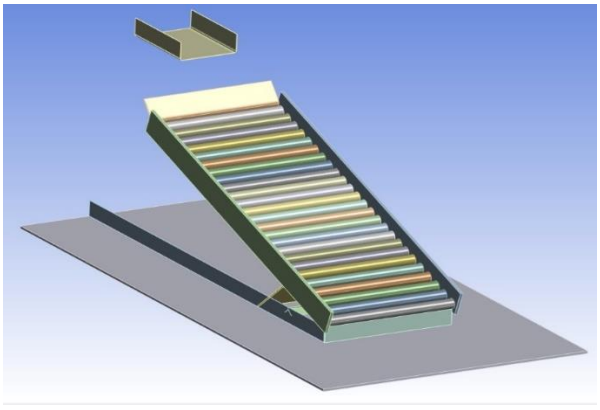

c). the roller screen with the deck angle of 19°.

Figure 13. Simulation of roller screens with various deck angles in ANSYS.

3. Results and discussion

Following the execution of DEM simulations across a range of operational conditions for the roller screen, the forces applied by the pellets on the rolls of the roller screen were simulated and quantified utilizing EDEM software. Subsequently, the simulation data were integrated with ANSYS software, in accordance with the algorithm illustrated in Figure 9, to conduct FEM simulations aimed at evaluating the influence of the roller screen's operational parameters on the mechanical behavior of the rolls. The findings from these simulations are detailed in the subsequent section.

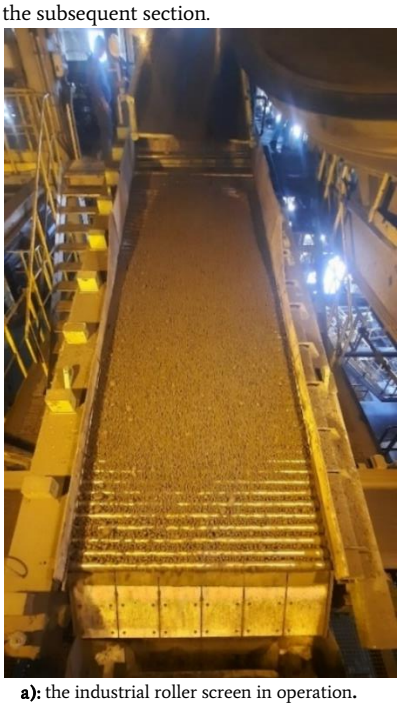

a): the industrial roller screen in operation.

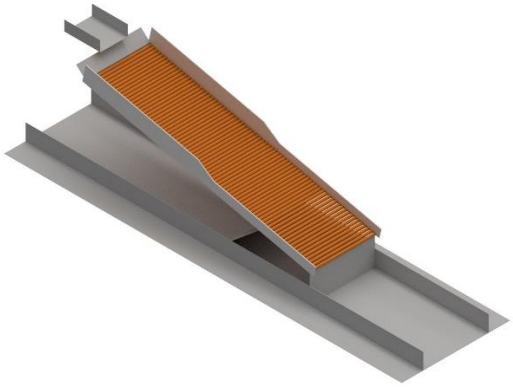

b): the geometry model of the industrial roller screen for the coupled DEM-FEM simulation.

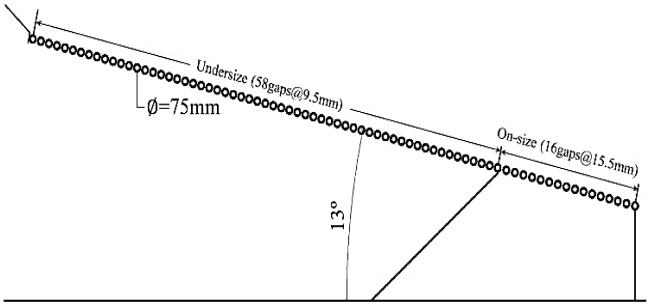

c). geometry specifications of the modeled industrial roller screen for simulation studies.

Figure 14. Geometry modeling of the industrial roller screen for simulation studies.

3.1. Investigating mesh independency and mesh metrics

To evaluate mesh independency, the geometry was meshed at 13 levels of refinement, and the results are presented in Figure 16. It is evident that further reducing the element dimensions from 2.25 mm and consequently increasing the number of mesh elements beyond 84438 does not significantly impact the simulation results for the equivalent stress. Specifically, when the element dimensions are increased from 1.25 mm to 1.75 mm and then to 2.25 mm, the number of elements decreased from 501444 to 189450 and 84438, respectively. The corresponding changes in the equivalent stress values range from 32.32 kPa to 33.19 kPa (i.e. a 2.71% increase) and 32.73 kPa (a 1.28 percent increase), respectively. Given that these changes are minimal, the dimensions of 2.25 mm and the count of 84438 elements were selected as the optimal parameters for meshing the roll based on the results of the mesh independence test. The corresponding mesh metric values are presented in Table 12.

3.2. Effect of the undersize gap

The outcomes of the simulation concerning the forces at different undersized gap values, as presented in Table 8, are depicted in Figure 17. Additionally, the simulation findings related to total deformation and equivalent stress are illustrated in Figure 18. The data indicate that a reduction in the undersized gap from 9.75 mm to 9 mm results in an increase in the average force, total deformation, and equivalent stress exerted on the rolls by 20.27%, 29.71%, and 102.91%, respectively.

Figure 19 depicts a pellet positioned between two adjacent rolls. This illustration indicates that the frictional force F_1, exerted by the front roll, facilitates the movement of the pellet by exerting an upward lifting action as it traverses the roller screen. In contrast, the frictional force F_2, applied by the rear roll, adversely affects the pellet's movement by exerting a downward pull, thereby causing the pellet to become more securely lodged within the interstitial space between the two rolls. A reduction in the gap between the rolls diminishes the likelihood of pellets, particularly those that are undersized, passing through, while simultaneously increasing the probability of their entrapment. This scenario heightens the likelihood of the pellet making contact with the surface of the rear roll, which results in the application of additional frictional forces, including F_2, in conjunction with force F_1. As a result, the average force exerted on the roll's surface by the pellets is amplified. A considerable proportion of the forces acting on the rolls, especially those situated in the central region of the roller screen and the final quarter which is distanced from the feed drop point, could be attributed to the frictional forces generated by the pellets located in the space between the two rolls.

Conversely, given that three-quarters of the screen's length and its associated rolls consist of the fine-grain area, the reduction of the undersize gap from 9.75 mm to 9.5 mm, 9.25 mm, and 9 mm, the probability of fine-grained pellets passing through the undersized area and subsequently leaving the roll surface is reduced. Consequently, the residence time on the roll surface is increased, which increases the likelihood of collisions with the roll surface and the potential for becoming lodged in the space between two consecutive rolls. This, in turn, increased the force exerted on the roll surface. This escalation in force subsequently contributes to a higher total deformation and equivalent stress.

3.3. Effect of rotational speed of the rolls

This section presents the findings from the DEM simulations and FEM analyses performed under the specified operating conditions detailed in Table 9. Figure 20 depicts the effects of alterations in the rotational speed of the rolls on the forces while Figure 21 illustrates the associated changes in the average values of total deformation and equivalent stress.

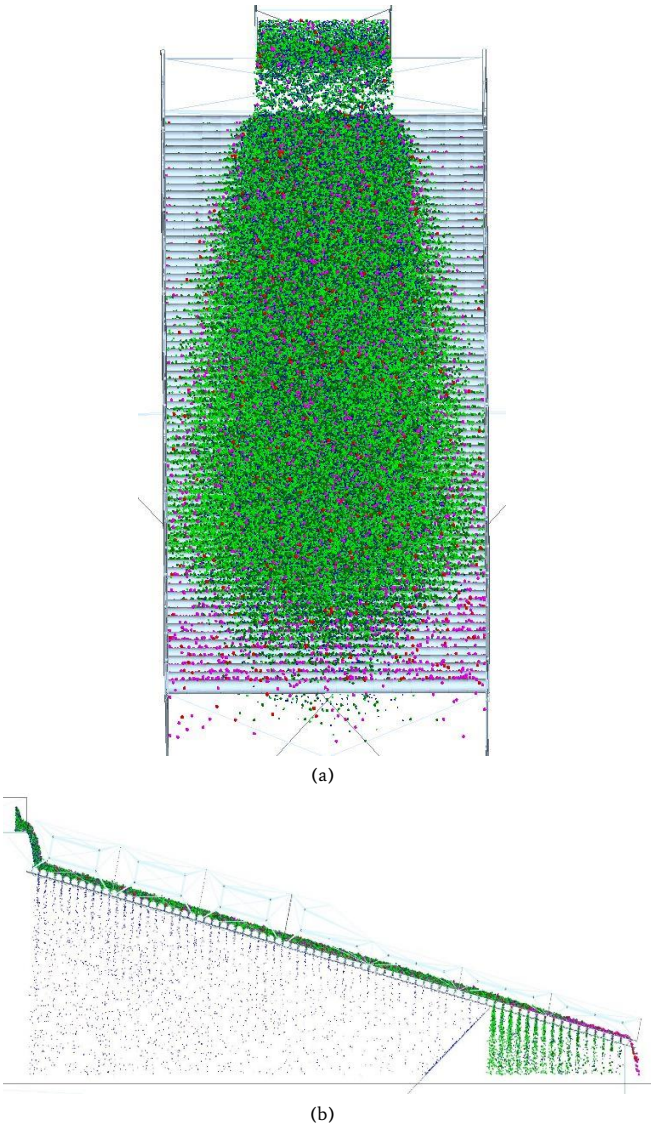

(a)

(b)

Figure 15. DEM simulation of the industrial roller screen by EDEM (in the steady state condition).

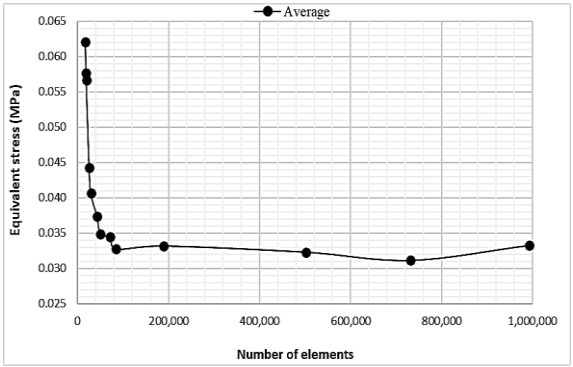

Figure 16. Analysis results of investigating mesh independency.

Table 11. Study on the industrial test effect on the coupled DEM-FEM simulation results of roller screen tests.

Deck angle (°D)	Roll speed (rpm)	Roll Dia. (mm)	Roll length (mm)	PU thickness (mm)	Undersize gap (mm)	Feed rate (t/h)
13	225	75	1800	10	9.5	120 and 200

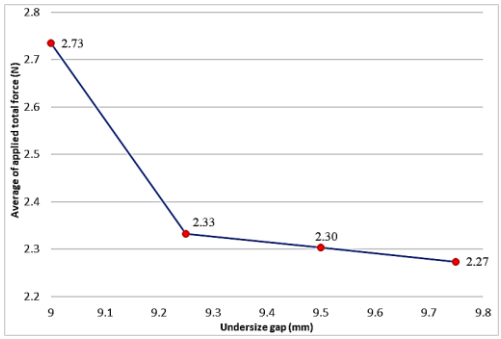

Figure 17. Study of the effect of the undersize gap on the applied force on rolls.

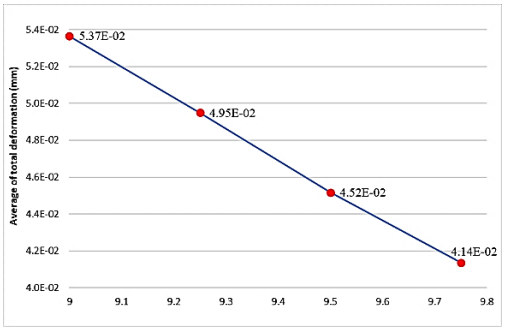

a). comparison of the effect of different values of the undersize gap on the average total deformation of rolls.

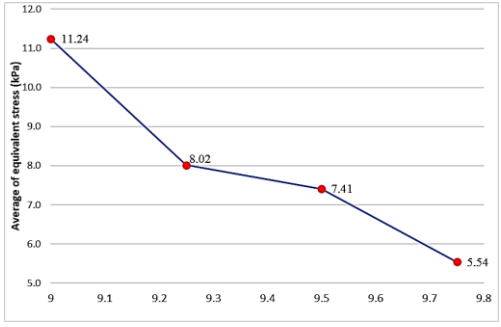

b). comparison of the effect of different values of the undersize gap on the average equivalent stress of rolls

Figure 18. Study of the effect of the undersize gap on the mechanical behavior of rolls.

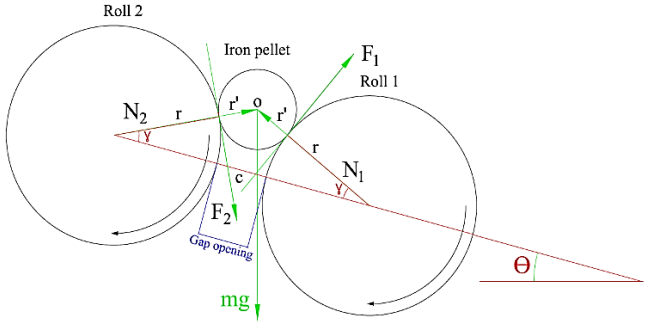

Figure 19. Applied forces on the stuck green pellet between two consecutive rolls.

where:

m = pellet mass (kg)

N1 and N2 = normal force (N)

F1 and F2 = friction force (N)

r = radius of the roll (m)

r' = radius of the pellet (m)

Θ = inclination angle of the roller screen (degree)

γ = the angle between the normal force vector and the inclination angle of the roller screen vector (degree)

g = gravitational acceleration (m/s2).

Table 12. Properties of the considered mesh for the FEM simulation of the rolls.

Parameter	Specification			
Mesh metrics	**Min**	**Max**	**Average**	**STD**
Element quality	0.8128	0.9879	0.9162	0.0472
Aspect ratio	1.1427	2.0275	1.5373	0.2494
Skewness	0.0279	0.3688	0.0567	0.0650
Orthogonal quality	0.9286	0.9998	0.9966	0.0093

The analysis indicates that a reduction in the rotational speed of the rolls from 300 rpm to 150 rpm leads to significant increases in various mechanical parameters: specifically, a 30.18% increase in average force, an 86.86% increase in total deformation, and a 56.24% increase in equivalent stress on the rolls. This phenomenon can be attributed to the decrease in angular momentum within the system formed by the interaction between the pellet and the roll surface which occurs when the rotational speed is lowered while maintaining constant parameters such as roll diameter, deck angle, and undersize gap. The diminished angular momentum results in a reduction of forward movement, thereby causing an accumulation of load on the rolls. Consequently, as time elapses, the pellets tend to remain in contact with the screen surface for extended periods, thereby increasing the probability of pellets becoming trapped between two adjacent rolls. This accumulation of force ultimately leads to an increase in both deformation and equivalent stress experienced by the rolls.

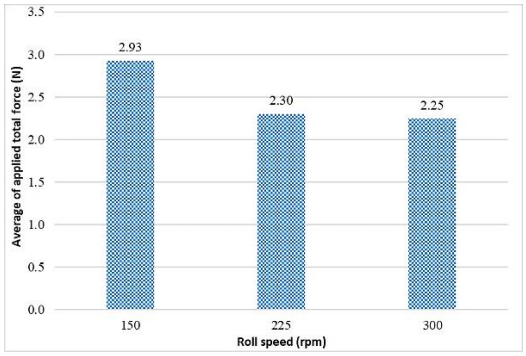

Figure 20. Study of the effect of the rotational speed of rolls on the average applied forces

3.4. Effect of deck angles

In Figure 22, the simulation outcomes depicting the forces exerted on the rolls at various deck angles are presented. Because the greatest distance exists between the feed transfer chute and the first roll of the screen, the first roll functions as an impact roll and experiences the highest forces. During the screening process, the behavior of the materials during random classification on the surface of the rolls, combined with the impact force and friction between consecutive rolls, enables the calculation of force values applied to each roll during the simulation using DEM simulation. Additionally, Figure 23 illustrates the simulation results concerning total deformation and equivalent stress. It is evident that a reduction in the deck angle from 19° to 10° results in increases in the average values of forces, total deformation, and equivalent stress on the rolls by 27.07%, 31.6%, and 19.85%, respectively. As demonstrated in Figure 19, a decrease in the deck angle of the roller screen (Θ) leads to a reduction in the gravitational force acting on the pellet along the screen (mg sin Θ). This decrease in force subsequently results in a lower pellet velocity. Moreover, a diminished deck angle of the roller screen prolongs the duration for which the pellets remain on

the surface of the rolls. Consequently, this increases the probability of pellets colliding with the rolls and enhances the likelihood of them becoming lodged between two consecutive rolls. Overall, these factors contribute to an increase in the applied forces which in turn leads to greater total deformation and equivalent stress.

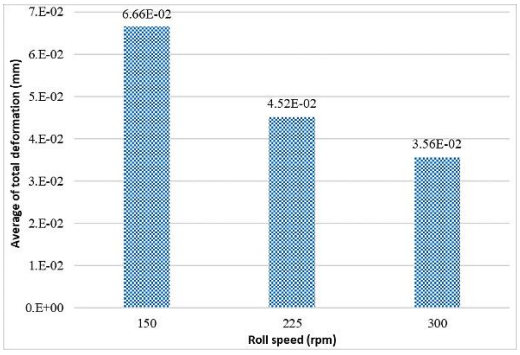

a). comparison of the effect of different values of the rotational speed of rolls on the average total deformation

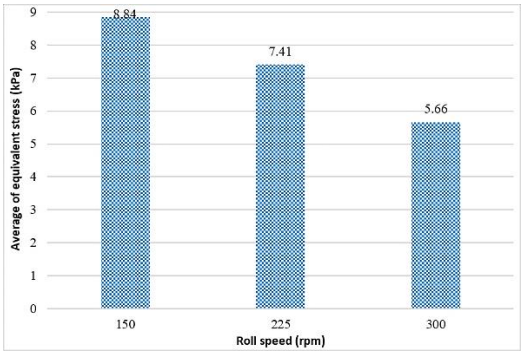

b) comparison of the effect of different values of the rotational speed of rolls on the average equivalent stress

Figure 21. Study of the effect of the rotational speed of rolls on their mechanical behavior.

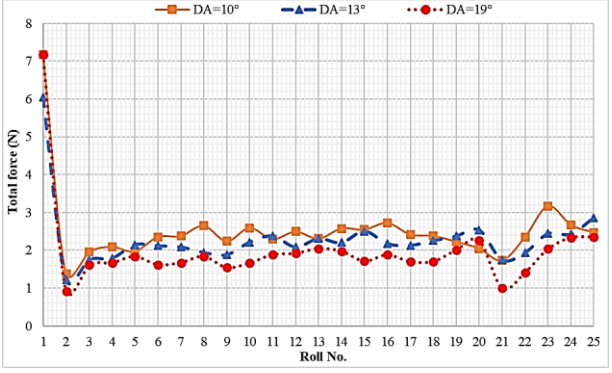

a). the effect of deck angle variations on the applied forces on rolls constituent of the roller screen

3.5. Industrial roller screening tests

Utilizing coupled DEM-FEM simulations, this study calculated the average total forces exerted on the various rolls of the industrial roller screen at two distinct feed capacities which constitutes a significant innovation of this research. The findings are depicted in Figure 24(a). Furthermore, Figure 24(b) provides a comparative analysis of the average forces experienced under the two specified industrial capacities against those recorded under laboratory conditions. The parameters for the laboratory roller screen test included a feeding capacity of 3.38 t/h, a deck angle of 13°, a roll rotational speed of 225 rpm, a roll diameter of 70 mm, and an undersized gap of 9.5 mm. As illustrated in Figure 25(b), the average force acting on the rolls of the laboratory roller screen is measured at 2.43 N. In contrast, simulations of a full-scale roller screen operating at capacities of 120 t/h and 200 t/h reveal average forces of 34.46 N and 54.06 N, respectively.

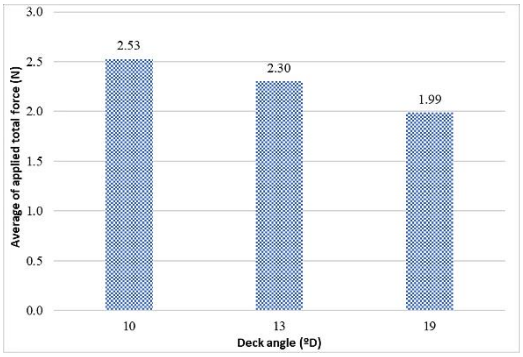

b). comparison of the effect of different values of deck angles on the average applied forces on rolls.

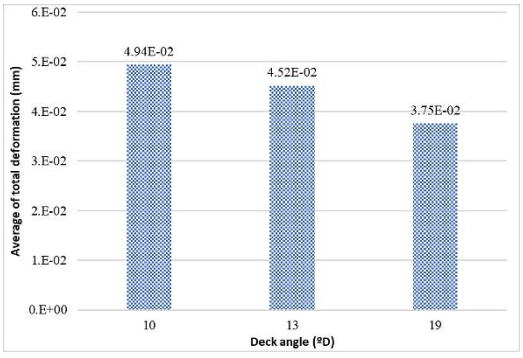

a): comparison of the effect of different values of deck angles on the average total deformation.

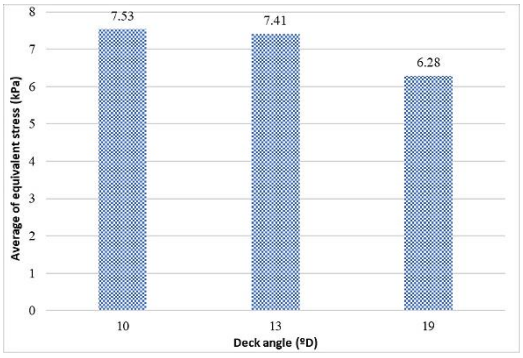

b). comparison of the effect of different values of deck angles on the average equivalent stress.

Figure 23. Study of the effect of deck angles on the mechanical behavior of rolls.

Subsequently, the computed force values were integrated into the FEM framework, allowing for the simulation of average total deformation and equivalent stress. The findings are illustrated in Figure 25, which also includes a comparison with the results obtained from the laboratory roller screen test. As illustrated in Figure 25(a), the average total deformation observed in the rolls of the laboratory roller screen is measured at 4.27E-05 mm. In contrast, under industrial conditions, this deformation increases significantly to 1.89E-02 mm at a processing capacity of 120 t/h, and further escalates to 2.95E-02 mm at a capacity of 200 t/h. In addition, Figure 25(b) indicates that the average equivalent stress exerted on the rolls of the laboratory roller screen is 1.79 kPa. However, in industrial environments, this stress rises markedly to 65.6

kPa at a capacity of 120 t/h and reaches 102.57 kPa at a capacity of 200 t/h. These findings underscore the influence of industrial-scale simulations and the corresponding increase in load capacity on both the total deformation and equivalent stress experienced by the rolls.

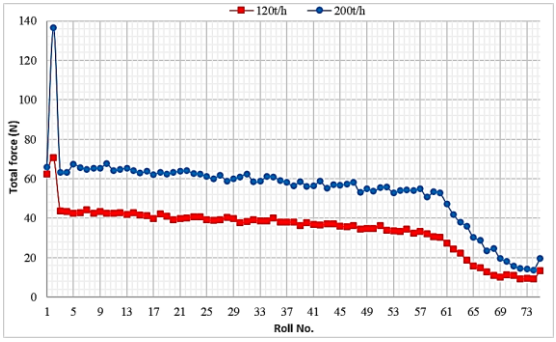

a). analysis results of the simulated total force.

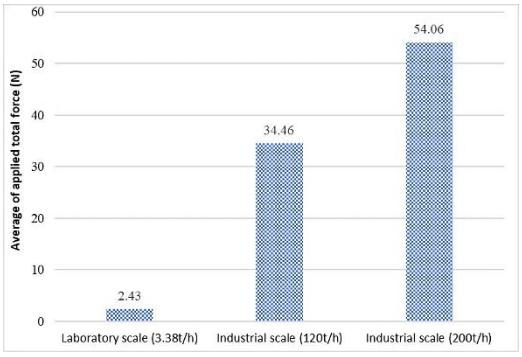

b). comparison of average of the applied total force for the industrial roller screen with the laboratory one.

Figure 24. Analysis results of the applied total force and torques on rolls of the industrial roller screen in feed rates of 120 and 200 t/h and comparison of their results with the laboratory test.

It is important to note that the forces applied to the rolls during both the laboratory and industrial tests are relatively low. Consequently, the resulting deformation and applied stress required a significant amount of time to manifest. To accurately assess the results of the simulation tests, it is essential to implement changes at an industrial scale, such as adjusting the fine grain gap, roll rotation speed, and screen deck angle on a roller screen. After a substantial period of screen operation, the results can be evaluated by examining the deformation and lifespan of the rolls as well as screen downtime. This evaluation can be conducted by comparing these metrics with the initial conditions prior to the changes, which will be the focus of authors' future research.

4. Conclusions

Through extensive coupled DEM-FEM simulation studies of the roller screen which employed a precisely modeled pellet shape and a hysteretic spring elastic-plastic contact model, the influence of the operating parameters of the roller screen on the force produced by the impact of the pellet, and subsequently, the mechanical behavior of the rolls, was examined. The following findings were obtained for the first time:

• The reduction of the undersize gap exerted an inverse effect on the force, total deformation, and equivalent stress experienced by the rolls. Notably, a decrease in the undersize gap from 9.75 mm to 9 mm led to an average increase in force of 20.27%, total deformation of 29.71%, and equivalent stress of 102.91% on the rolls. Consequently, to reduce the deformation of the rolls and alleviate their adverse effects on the efficiency of the roller screen, an optimal value of the undersize gap must be determined to balance its influence on roll deformation and overall efficiency.

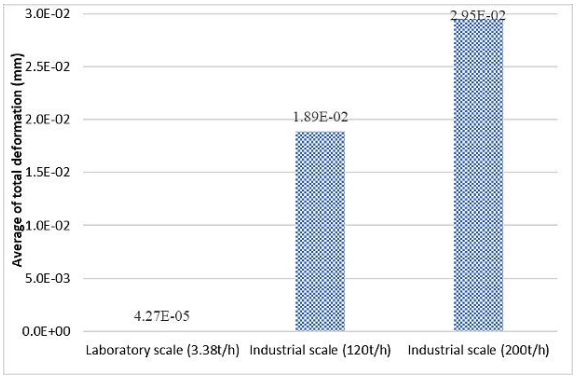

a). analysis results of simulated total deformation.

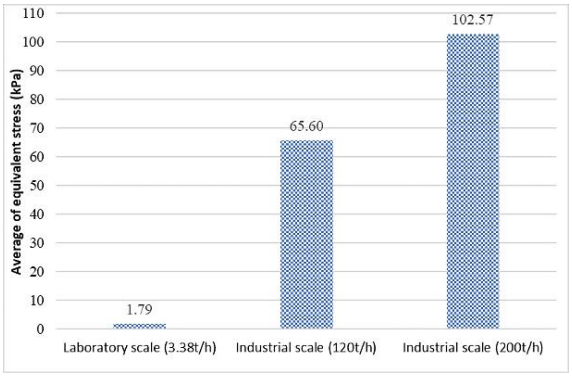

b). analysis results of simulated equivalent stress.

Figure 25. Analysis results of the mechanical behavior of rolls of the industrial roller screen in feed rates of 120 and 200 t/h and comparison of their results with the laboratory test.

• A reduction in the rotational speed of the rolls resulted in an increase in the force, total deformation, and equivalent stress experienced by the rolls. Specifically, when the rotational speed decreased from 300 rpm to 150 rpm, the average force, total deformation, and equivalent stress applied to the rolls exhibited increases of 30.18%, 86.86%, and 56.24%, respectively.

• The angle of the roller screen's deck exhibited an inverse correlation with the force, total deformation, and equivalent stress experienced by the rolls. Notably, a reduction in the deck angle from 19° to 10° resulted in enhancements in the average measurements of force, total deformation, and equivalent stress by 27.07%, 31.6%, and 19.85%, respectively.

• Coupled DEM-FEM simulations of the roller screen were performed at an industrial scale, examining two distinct feed capacities: 120 t/h and 200 t/h. The outcomes of these simulations were compared with results derived from laboratory roller screen tests conducted at a feed capacity of 3.38 t/h, utilizing the same roll diameter. In the laboratory experiments, the average measurements for total force, total deformation, and equivalent stress were recorded at 2.43 N, 4.27E-05 mm, and 1.79 kPa, respectively. Conversely, at the industrial scale with a feed capacity of 120 t/h, these parameters escalated to 34.46 N, 1.89E-02 mm, and 65.6 kPa. When the feed capacity increased to 200 t/h, the values further rose to 54.06 N, 2.95E-02 mm, and 102.57 kPa. These results underscore the significant impact of both feed capacity and full-scale simulation on the total force, deformation, and stress experienced by the rolls in the roller screen system.

References

[1] R.M. Carvalho, A.D. Thomazini, E.R. Cunha, B.B. e Silva, L.M. Tavares, Simulation of Classification and Stratification in Double-Deck Roller Screening of Green Iron Ore Pellets using

DEM, Trans. Indian Inst. Met. (2023). https://doi.org/10.1007/s12666-023-02958-6.

[2] M. Javaheri, A. Jafari, G.H. Baradaran, A. Saidi, Effects of rollers speed regime on the roller screen efficiency, Miner. Process. Extr. Metall. Rev. 43 (2022) 648–655.

[3] A.G. Andrade, S. Beaudin, M. Athayde, Impact of key parameters on the iron ore pellets roller screening performance, Metall. Res. Technol. 119 (2022) 311. https://doi.org/10.1051/metal/2022045.

[4] X.D. Yang, L. La Zhao, H.X. Li, C.S. Liu, E.Y. Hu, Y.W. Li, Q.F. Hou, DEM study of particles flow on an industrial-scale roller screen, Adv. Powder Technol. 31 (2020) 4445–4456. https://doi.org/10.1016/j.apt.2020.09.020.

[5] B.B. e Silva, E.R. Cunha, R.M. Carvalho, L.M. Tavares, Modeling and simulation of green iron ore pellet classification in a single deck roller screen using the discrete element method, Powder Technol. 332 (2018) 359–370. https://doi.org/10.1016/j.powtec.2018.04.005.

[6] S.K. Kawatra, V. Claremboux, Iron ore pelletization: Part i. Fundamentals, Miner. Process. Extr. Metall. Rev. 43 (2022) 529–544.

[7] F.P. Beer, E.R. Johnston, J.T. DeWolf, D.F. Mazurek, Mechanics of materials (Eighth), (2020).

[8] R.G. Budynas, J.K. Nisbett, Shigley's mechanical engineering design, McGraw-Hill New York, 2011.

[9] W.F. Hosford, Mechanical behavior of materials, Cambridge university press, 2010.

[10] M.A. Meyers, K.K. Chawla, Mechanical Behavior of Materials, Cambridge University Press, 2009.

[11] B.B. e Silva, E.R. da Cunha, R.M. de Carvalho, L.M. Tavares, Improvement in Roller Screening of Green Iron Ore Pellets by Statistical Analysis and Discrete Element Simulations, Miner. Process. Extr. Metall. Rev. 41 (2019) 323–334. https://doi.org/10.1080/08827508.2019.1635473.

[12] M. Javaheri, A. Jafari, G.H. Baradaran, A. Saidi, Effects of Rollers Speed Regime on the Roller Screen Efficiency, Miner. Process. Extr. Metall. Rev. 00 (2021) 1–8. https://doi.org/10.1080/08827508.2021.1916926.

[13] G.K.P. Barrios, R.M. De Carvalho, A. Kwade, L. Marcelo, Contact parameter estimation for DEM simulation of iron ore pellet handling, Powder Technol. (2013) 1–10. https://doi.org/10.1016/j.powtec.2013.01.063.

[14] J. Cheng, T. Ren, Z. Zhang, D. Liu, X. Jin, A dynamic model of inertia cone crusher using the discrete element method and multi-body dynamics coupling, Minerals. 10 (2020) 1–23. https://doi.org/10.3390/min10100862.

[15] D. Xu, Y. Shen, A novel CFD-DEM-DPM modelling of fluid-particles-fines reacting flows, Chem. Eng. Sci. 292 (2024) 120014. https://doi.org/10.1016/j.ces.2024.120014.

[16] Z.J. Yang, X. Lian, C. Savari, M. Barigou, Evaluating the effectiveness of CFD-DEM and SPH-DEM for complex pipe flow simulations with and without particles, Chem. Eng. Sci. 288 (2024) 119788. https://doi.org/10.1016/j.ces.2024.119788.

[17] C.L. Alves, V. Skorych, A. Noni Jr, D. Hotza, S.Y.G. González, S. Heinrich, Microscale DEM simulation of spray-dried porcelain granules under unia xial compaction, Powder Technol. 428 (2023) 118863.

[18] C.L. Alves, S. Heinrich, Improving the analysis of heat transfer in packed beds: A comparative study between DEM simulations and existing literature models, Chem. Eng. Res. Des. 203 (2024) 357–367. https://doi.org/10.1016/j.cherd.2024.01.062.

[19] M. Moncada, F. Betancourt, C.G. Rodríguez, P. Toledo, Effect of Particle Shape on Parameter Calibration for a Discrete Element Model for Mining Applications, Minerals. 13 (2023) 1–17. https://doi.org/10.3390/min13010040.

[20] H. Long, C.Z. Huang, D.C. Li, Dynamic analysis of beam structure of linear vibrating screen, AIP Adv. 14 (2024). https://doi.org/10.1063/5.0182353.

[21] N.I.E. Zhiheng, Dynamic characteristic analysis of vibration screen based on joint face analysis, J. Phys. Conf. Ser. 2085 (2021). https://doi.org/10.1088/1742-6596/2085/1/012013.

[22] H. Khoshdast, H. Khoshdast, S. Jalilifard, Dynamic analysis of a dashpots equipped vibrating screen using finite element method, Physicochem. Probl. Miner. Process. 57 (2020) 112–126. https://doi.org/10.37190/ppmp/130001.

[23] N. Xu, X. Wang, D. Lin, W. Zuo, Numerical Simulation and Optimization of Screening Process for Vibrati ng Flip-Flow Screen Based on Discrete Element Method–Finite Element Me thod–Multi-Body Dynamics Coupling Method, Minerals. 14 (2024). https://doi.org/10.3390/min14030278.

[24] A. Öchsner, Elasto-plastic Finite Element Simulations, Elem. Class. Plast. Theory. (2022) 61–101. https://doi.org/10.1007/978-3-031-14201-7_4.

[25] X. Sun, Y. Sui, Y. Zheng, L. Wang, H. Zhu, Finite element analysis and optimization design of large vibrating screen based on equivalent static load method, Eng. Res. Express. 6 (2024). https://doi.org/10.1088/2631-8695/ad3520.

[26] J.C. Yu, J.T. Wang, J.W. Pan, N. Guo, C.H. Zhang, A dynamic FEM-DEM multiscale modeling approach for concrete structures, Eng. Fract. Mech. 278 (2023) 109031. https://doi.org/10.1016/j.engfracmech.2022.109031.

[27] Q. Zhou, W.J. Xu, R. Lubbe, Multi-scale mechanics of sand based on FEM-DEM coupling method, Powder Technol. 380 (2021) 394–407. https://doi.org/10.1016/j.powtec.2020.11.006.

[28] F. Ye, Y. Qiang, W. Jiang, X. Fu, Dem–fem coupling simulation of the transfer chute wear with the dynami c calibration dem parameters, Processes. 9 (2021). https://doi.org/10.3390/pr9101847.

[29] X. Yang, D. Wu, Y. Bai, H. Chen, X. Wang, Identification of force chains in wet coal dust layer and the effect of porosity on three-body contact stiffness, Sci. Rep. 14 (2024). https://doi.org/10.1038/s41598-024-67340-y.

[30] H. Cheng, A.R. Thornton, S. Luding, A.L. Hazel, T. Weinhart, Concurrent multi-scale modeling of granular materials: Role of coarse-graining in FEM-DEM coupling, Comput. Methods Appl. Mech. Eng. 403 (2023) 115651. https://doi.org/10.1016/j.cma.2022.115651.

[31] X. Hou, W. Wang, J. Pan, P. Mao, S. Zhang, C. Duan, Optimization of flip-flow screen plate based on DEM-FEM coupling model and screening performance of fine minerals, Miner. Eng. 211 (2024) 108694. https://doi.org/https://doi.org/10.1016/j.mineng.2024.108694.

[32] G. Zhao, K. Pu, N. Xu, S. Gong, X. Wang, Simulation of particles motion on a double vibrating flip-flow screen surface based on FEM and DEM coupling, Powder Technol. 421 (2023) 118422. https://doi.org/https://doi.org/10.1016/j.powtec.2023.118422.

[33] N. Xu, C. Yu, S. Gong, G. Zhao, D. Lin, X. Wang, Numerical study and multi-objective optimization of flexible screening process of flip-flow screen: A DEM-FEM approach, Adv. Powder Technol. 33 (2022) 103650. https://doi.org/https://

doi.org/10.1016/j.apt.2022.103650.

[34] H. Xia, X. Tong, Z. Li, X. Wu, DEM-FEM coupling simulations of the interactions between particles and screen surface of vibrating screen, Int. J. Min. Miner. Eng. 8 (2017) 250–263. https://doi.org/10.1504/IJMME.2017.085841.

[35] Z. Wang, L. Peng, C. Zhang, L. Qi, C. Liu, Y. Zhao, Research on impact characteristics of screening coals on vibrating screen based on discrete-finite element method, Energy Sources, Part A Recover. Util. Environ. Eff. 42 (2020) 1963–1976. https://doi.org/10.1080/15567036.2019.1604905.

[36] Z. Wang, C. Liu, J. Wu, H. Jiang, Y. Zhao, Impact of screening coals on screen surface and multi-index optimization for coal cleaning production, J. Clean. Prod. 187 (2018) 562–575. https://doi.org/10.1016/j.jclepro.2018.03.238.

[37] H. Zhang, X. Zheng, W. Jing, Numerical investigation on dynamic response of the screen mesh in vibrating screening through DEM-FEM co-simulation, Particuology. 87 (2024) 205–217. https://doi.org/10.1016/j.partic.2023.08.013.

[38] L. Peng, Z. Wang, W. Ma, X. Chen, Y. Zhao, C. Liu, Dynamic influence of screening coals on a vibrating screen, Fuel. 216 (2018) 484–493. https://doi.org/10.1016/j.fuel.2017.12.041.

[39] Altair EDEM software, EDEM 2021.2 Documentation, (2022).

[40] M. Asghari, M. Noaparast, M. Jahani, Implementation of DEM to calibrate contact parameters, as a novel simulation of the elastoplastic behavior of green iron pellet classified by roller screen, Adv. Powder Technol. 35 (2024) 104457. https://doi.org/https://doi.org/10.1016/j.apt.2024.104457.